August 27-31, 2023
FLORENCE - ITALY
ICWE 16
16th International Conference on Wind Engineering

Towards high-fidelity large-eddy simulation of extreme wind/wave events in coastal regions

Hanul Hwang[1] and Catherine Gorlé[1,2]

[1]*Center for Turbulence Research, Stanford, USA, hanul@stanford.edu*
[2]*Stanford University, Stanford, USA, gorle@stanford.edu*

SUMMARY:
The impacts of climate-driven hazards in coastal regions escalate due to sea level rise and anthropogenic warming, causing severe direct losses and fatalities. To support research on mitigating the impacts of these hazards, the NICHE team aims to design a full-scale testing infrastructure for extreme wind and wave events. This study presents progress towards establishing validated high-fidelity large-eddy simulations (LES) of coupled wind and wave problems to inform the design of NICHE. We demonstrate the performance of the widely-used opensource code OpenFOAM for wind/wave simulations with moderate wind speeds. Also, the sensitivity of such simulations on boundary conditions and turbulent models is discussed.

Keywords: wind/wave, turbulence, LES

1. MOTIVATION AND OBJECTIVE

With coastal communities becoming increasingly susceptible to extreme climate-driven hazards, there is a pressing need to improve resilience and reduce the impact of these hazards. To support research on enhancing the resilience of communities to such extreme events, the NICHE[1] team aims to design a full-scale testing infrastructure to model the impacts of wind and coastal hazards. The design of the facility will rely on physical experiments as well as numerical simulations.

Computational modeling of the effects of simultaneous action of wind and waves on structures has a high level of complexity, since combined wind and wave flow is a multiphysics and multiscale problem. Thus, prior studies are often limited to simplified scenarios. First, considering the interaction between wind and waves, wave-induced turbulent structures have been extensively studied (Husain et al., 2022; Sullivan et al., 2000; Yang and Shen, 2010), and, informed by wave generation theories, numerical studies of the wind-driven wave generation are an active area of research (Lin et al., 2008; Wu and Deike, 2021; Zonta et al., 2015). However, most of the research assumes periodic domains with small wave amplitudes and low wind speeds. Turbulence is assumed statistically stationary, missing non-equilibrium turbulence effects on wave evolution (Hao and Shen, 2022). Next, considering the interaction between wind, waves, and structures, a few coupled wave/wind simulations have been reported for offshore wind turbine dynamics (Liu et al.,

[1]National full-scale testing infrastructure for community hardening in extreme wind, surge, and wave events (NICHE)

2017; Ren et al., 2014). For coastal infrastructure, the impact of waves has been investigated without wind effect or wave breaking (Hayatdavoodi et al., 2015; Huang et al., 2009; Meng, 2008; Park et al., 2018). Hence, there is a need to consider computational modeling of coastal wind/wave processes that include the effect of a spatial variation of the bathymetry on the wind/wave dynamics and their interaction with structures.

In this study, we demonstrate the capability of the widely-used open source code OpenFOAM for performing large-eddy simulations (LES) of a combined wind/wave flow through experimental validation. Sensitivities of the simulations to various model choices, such as boundary conditions, turbulence model, and mesh, are reported. Based on the results, further steps to advance towards model validation for coastal wind/wave dynamics will be defined.

2. METHODS

2.1. Simulation setup

The simulations reproduce the experiment reported in Buckley and Veron (2016). We consider a rectangular domain of length 1.5m, width 0.1m, and height 2.62m. For the air-side inlet, a divergence-free synthetic eddy method (Poletto et al., 2013) is used to introduce a realistic turbulent boundary layer that matches the experimental mean log-law profile. Experimental information on the turbulence intensity in the air inlet is not available, so a default turbulence intensity of 16% is used, and sensitivity to this input parameter is investigated by performing a simulation with a higher turbulence intensity of 23%. For the water side, Stokes waves of wave height 0.1m, wavelength 0.25m and water depth 2.51m are introduced. A pressure inlet-outlet condition and wave absorption outlet condition are employed for the air and water outlets, respectively. A periodic boundary condition is prescribed at the side walls. Slip and no-slip boundary conditions are imposed at the top and bottom boundary, respectively.

A grid dependency study revealed a strong sensitivity of the solution to the grid resolution near the interface. To obtain accurate results, the results presented in this abstract were obtained with a grid that is refined near the interface down to $y^+ = 2$, which is 0.0002m in cell height. The influence of the subgrid model is investigated by comparing simulations with three different models: the k-equation model, the Smagorinsky model, and the WALE model.

The simulations use an algebraic volume-of-fluid (VOF) method with MULES flux limiter for interface capturing. The volume fraction of one of the fluids is represented by the phase indicator ϕ. The transport equation for ϕ is given as

$$\frac{\partial \phi}{\partial t} + \vec{\nabla} \cdot (\vec{u}\phi) = u_c \phi (1-\phi), \tag{1}$$

where t and u_c indicate the time and compression velocity, which controls the thickness of interfaces, respectively. $\vec{u}$ denotes the velocity vector.

2.2. Quantities of interest

Comparison between experimental and LES results is performed by decomposing the velocity field $\mathbf{u}$ into three parts: wave-independent, wave-coherent, and pure-turbulent components:

$$\mathbf{u}(x,y,z,t) = \overline{\mathbf{u}}(\zeta) + \widetilde{\mathbf{u}}(\xi,\zeta) + \mathbf{u}'(x,y,z,t), \tag{2}$$

where x, y, z and t are Cartesian coordinates and time, respectively. (ξ, ζ) is the wave-following coordinate system. $\overline{\mathbf{u}}$ represents wave-independent portion. $\widetilde{\mathbf{u}}$ and $\mathbf{u}'$ refer to wave-coherent part and pure-turbulence part, respectively (Buckley and Veron, 2016).

3. RESULTS

3.1. Turbulence over waves

Figure 1(a) shows a snapshot of the predicted field velocity. Following Eq. (2), the velocity field is decomposed into three components, and the wave-coherent component is illustrated in Figure 1(b), showing the acceleration over the wave crest and the deceleration towards the trough.

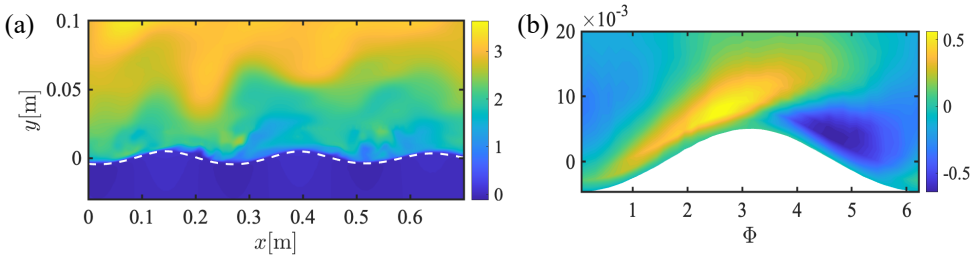

Figure 1. (a) Instantaneous velocity field. (b) Wave-coherent component of the velocity field. White dashed-line denotes the interface.

Figure 2 compares the wave-independent mean velocity as well as the wave-coherent and pure-turbulent Reynolds stress from the different simulations and the experiments. For fixed boundary conditions, no discernible difference is observed for the different subgrid models. However, when changing the turbulent inlet condition, we see significant changes in the Reynolds stress near the interface on and grid resolution (see the red and purple lines in Figure 2). This sensitivity indi-

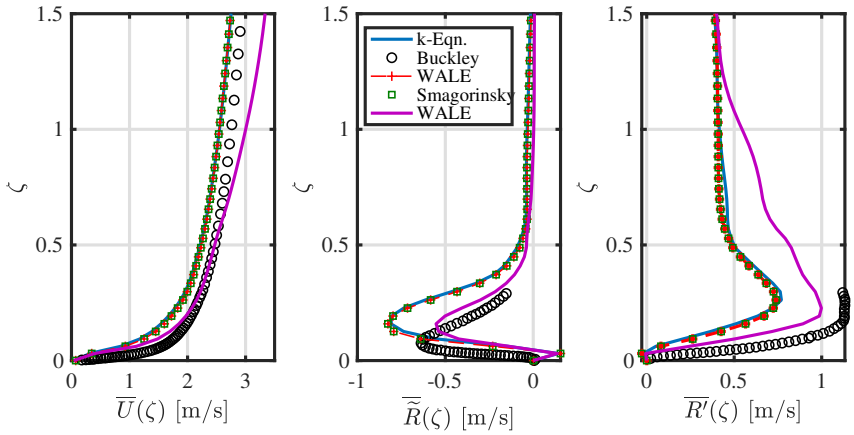

Figure 2. Comparison of simulation and experimental results. From left to right, wave-independent mean velocity, wave-coherent Reynolds stress, and pure-turbulent Reynolds stress. Symbols and lines indicate different turbulent models: blue (k–equation), red-plus (WALE), square (Smagorinsky), and purple (WALE, inlet condition with higher turbulence). Circles refer to the experimental data.

cates the importance of accurately characterizing the turbulence in the incoming wind field in the experiments if the data has to support CFD model validation.

4. CONCLUSIONS

The capability of the open-source code OpenFOAM for wind/wave simulations has been demonstrated through comparison with experimental data for a simplified configuration. However, the turbulence in the wind field near the interface was found to be highly sensitive to the boundary conditions for the air phase. Furthermore, the simulations required a fine grid near the interface, which results in a significant computational cost even for moderate wind speeds. To support future validation of wind/wave simulations for higher wind speeds and wave heights in near-shore environments, experiments should carefully measure and report the inlet conditions for both the water and the air phases, while simulations should explore using interface schemes that can handle coarser mesh resolutions.

ACKNOWLEDGEMENTS

This study was supported by funding from the National Science Foundation under grant CMMI-21311961.

REFERENCES

Buckley, M. P. and Veron, F., 2016. Structure of the airflow above surface waves. Journal of Physical Oceanography 46, 1377–1397.

Hao, X. and Shen, L., 2022. Large-eddy simulation of gusty wind turbulence over a travelling wave. Journal of Fluid Mechanics 946, A8.

Hayatdavoodi, M., Seiffert, B., and Ertekin, R. C., 2015. Experiments and calculations of cnoidal wave loads on a flat plate in shallow-water. Journal of Ocean Engineering and Maritime Energy 1 (1), 77–99.

Huang, W., Xiao, H., Bryan, G., and Rotunno, R., 2009. Numerical modeling of dynamic wave force acting on Ecambia bay bridge deck during hurricane Ivan. Journal of Waterway, Port, Coastal, and Ocean Engineering 135 (4), 164–175.

Husain, N. T., Hara, T., and Sullivan, P. P., 2022. Wind turbulence over misaligned surface waves and air–sea momentum flux. Part I: waves following and opposing wind. Journal of Physical Oceanography 52, 119–139.

Lin, M.-Y., Moeng, C.-H., Tsai, W.-T., Sullivan, P. P., and Belcher, S. E., 2008. Direct numerical simulation of wind-wave generation processes. Journal of Fluid Mechanics 616, 1–30.

Liu, Y., Xiao, Q., Incecik, A., Peyrard, C., and Wan, D., 2017. Establishing a fully coupled CFD analysis tool for floating offshore wind turbines. Renewable Energy 112 (280-301).

Meng, B., 2008. Calculation of extreme wave loads on coastal highway bridges.

Park, H., Do, T., Tomiczek, T., Cox, D. T., and Lindt, J. W. van de, 2018. Numerical modeling of non-breaking, impulsive breaking, and broken wave interaction with elevated coastal structures: laboratory validation and inter-model comparisons. Ocean Engineering 158, 78–98.

Poletto, R., Craft, T., and Revell, A., 2013. A new divergence free synthetic eddy method for the reproduction of inlet flow conditions for LES. Flow, turbulence and combustion 91, 519–539.

Ren, N., Li, Y., and Ou, J., 2014. Coupled wind-wave time domain analysis of floating offshore wind turbine based on computational fluid dynamics method. Journal of Renewable and Sustainable Energy 6 (2).

Sullivan, P. P., McWilliams, J. C., and Moeng, C.-H., 2000. Simulation of turbulent flow over idealized water waves. Journal of Fluid Mechanics 404, 47–85.

Wu, J. and Deike, L., 2021. Wind wave growth in the viscous regime. Physical Review Fluids 6, 094801.

Yang, D. and Shen, L., 2010. Direct-simulation-based study of turbulent flow over various waving boundaries. Journal of Fluid Mechanics 650, 131–180.

Zonta, F., Soldati, A., and Onorato, M., 2015. Growth and spectra of gravity–capillary waves in countercurrent air/water turbulent flow. Journal of Fluid Mechanics 777, 245–259.